

Transductive Reward Inference on Graph

Bohao Qu, Xiaofeng Cao, *Member, IEEE*, Qing Guo, *Member, IEEE*, Chang Yi, *Senior Member, IEEE*,
Ivor W. Tsang, *Fellow, IEEE* and Chengqi Zhang, *Senior Member, IEEE*

Abstract—In this study, we present a transductive inference approach on that reward information propagation graph, which enables the effective estimation of rewards for unlabelled data in offline reinforcement learning. Reward inference is the key to learning effective policies in practical scenarios, while direct environmental interactions are either too costly or unethical and the reward functions are rarely accessible, such as in healthcare and robotics. Our research focuses on developing a reward inference method based on the contextual properties of information propagation on graphs that capitalizes on a constrained number of human reward annotations to infer rewards for unlabelled data. We leverage both the available data and limited reward annotations to construct a reward propagation graph, wherein the edge weights incorporate various influential factors pertaining to the rewards. Subsequently, we employ the constructed graph for transductive reward inference, thereby estimating rewards for unlabelled data. Furthermore, we establish the existence of a fixed point during several iterations of the transductive inference process and demonstrate its at least convergence to a local optimum. Empirical evaluations on locomotion and robotic manipulation tasks validate the effectiveness of our approach. The application of our inferred rewards improves the performance in offline reinforcement learning tasks.

Index Terms—Reward propagation graph, reward inference, offline reinforcement learning.

I. INTRODUCTION

OFFLINE reinforcement learning (RL) problems can be defined as a data-driven formulation of the reinforcement learning problem, that is, learning a policy from a fixed dataset without further environmental input [1], [2], [3]. Reliable and effective offline RL methods would significantly affect various fields, including robots [4], [5], autonomous driving [6], recommendation systems [7], [8], and healthcare [9]. Rewards are typically necessary for learning policies in offline RL, but they are rarely accessible in practice, and the rewards for state-action pairs need to be manually annotated, which is difficult and time-consuming. Meanwhile, real-world offline RL datasets always have a small amount with reward and a large amount always without reward. Thus, learning a model from limited data with rewards to label unrewarded data is

critical for learning effective policies to apply offline RL to various applications.

Typical methods have attempted various types of supervision for reward learning. The method proposed by [10] and ORIL [11] learns reward functions and uses them in offline RL. [10] employs a reward sketching interface to elicit human preferences and use them as a signal for learning. In reward sketching, the annotator draws a curve where higher values correspond to higher rewards. ORIL [11] relies on demonstrated trajectories to obtain reward functions both from labelled and unlabelled data at the same time as training an agent. [12] propose the timestep annotations are binary and treat the reward prediction as a classification problem to focus on sample efficiency with limited human supervision.

Reward learning for offline RL is roughly divided into two categories: timestep-level (e.g., state-action pair reward annotations for the entire episode produced by humans [10]) and episode-level supervision (e.g., annotations of success for the whole episode [12], [11]). For episode-level supervision, [12] assumes rewards are binary, and it indicates if the task is solved. Episode annotations provide only limited information about the reward. They indicate that some of the state-action pairs from the episodes show successful behavior but do not indicate when the success occurs. So the episode-level supervision method is not adaptation to any value reward learning question. For timestep-level annotations, [12] and [13] need first to annotate demonstrated trajectories that are the successful trajectories (e.g., expert demonstrations). [10] employs a reward sketching interface to elicit human preferences and use them as a signal for learning, but the method is hard to solve tasks where variable speed is important or with cycles as in walking. Accordingly, existing methods are unsuitable for timestep-level reward learning with arbitrary values in offline reinforcement learning without any expert trajectories. The manual annotation of rewards for state-action pairs is costly, making it challenging to learn effective policies with limited reward labelled data. This makes it challenging to apply offline reinforcement learning to a variety of scenarios.

In a general sense, offline RL addresses the problem of learning to control a dynamic system, which is fully defined by a Markov decision process (MDP). An MDP is a sequential decision process for state-to-state transitions, which could be formed as a chain, and multiple chains of multiple MDPs can be combined to form a graph. In the graph, each node represents a state-action pair, and each edge is labelled with the probability of transitioning from one state to another state, given a particular action. The graph possesses the contextual properties of information propagation, the structure is characterized by connectivity, where each node is connected to multiple other nodes. It is convenient to perform inference through a message

Bohao Qu, Xiaofeng Cao, and Yi Chang are with the School of Artificial Intelligence, Jilin University, Changchun, Jilin 130012, China, and also with the Engineering Research Center of Knowledge-Driven Human-Machine Intelligence, Ministry of Education, China.

E-mail: qubohao@126.com, {xiaofengcao, yichang}@jlu.edu.cn.

Ivor W. Tsang and Qing Guo are with the A*STAR Centre for Frontier AI Research, Singapore 138632, and Ivor W. Tsang is also with the Australian Artificial Intelligence Institute, University of Technology Sydney, Ultimo, NSW 2007, Australia.

E-mail: {Ivor_Tsang, guo_qing}@cfar.a-star.edu.sg.

Chengqi Zhang is with the Australian Artificial Intelligence Institute, University of Technology Sydney, Ultimo, NSW 2007, Australia. E-mail: chengqi.zhang@uts.edu.au.

Manuscript created January, 2024.

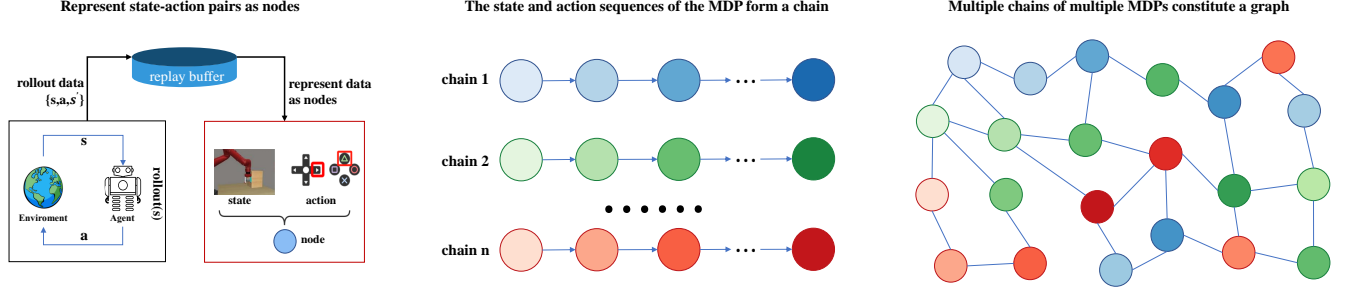


Fig. 1. We first represent each state-action pair within a Markov decision process (MDP) as an individual graph node. Then, we establish a foundation for modeling the state-action sequences across multiple MDPs as interconnected chains. Finally, these chains collectively form a comprehensive graph that encapsulates the dynamics of multiple MDPs. The graph structure is characterized by connectivity, where each node is connected to multiple other nodes. We leverage this feature to propagate reward-related information within the graph.

passing mechanism, and the inference procedure essentially propagates information from the state-action pairs with rewards to the state-action pairs without rewards and results in a reward function over state-action pairs, as shown in Fig. 1. Meanwhile, the label-efficiency problem has been successfully addressed through label propagation (LPA) approaches [14], [15], [16], [17], [18], [19], [20], [21] which is based on graph models and plays a significant role in leveraging unlabelled dataset to improve the model performance with low cost. Label propagation approaches formulate labelled and unlabelled data as a graph structure, where nodes represent sample data and edges represent relationships between nodes, and the node labels are propagated and aggregated along the edges.

Inspired by the label propagation approaches, we present TRAIN: **Tr**ansductive **R**ewards **I**nfere**n**ce with **P**ropagation **G**raph for **O**ffline **R**einforcement **L**earning. Transduction is reasoning from observed training cases to test cases. We learn from the already observed state-action pairs with rewards and then predict the state-action pairs without rewards. Even though we do not know the rewards of most state-action pairs, we can leverage the graph structure established by MDPs to propagate limited reward information. To be specific, TRAIN consists of the following key ingredients:

- (a) **Reward Propagation Graph:** We represent each state-action pair as a graph node and leverage the similarities and relationships between them to learn the edge weights of the nodes. It is worth noting that rewards are influenced by many factors, and all of the factors should be considered when learning the reward propagation graph.
- (b) **Transductive Reward Inference:** We employ the reward propagation graph to infer rewards for state-action pairs that are without rewards and then utilize them for doing offline RL. The reward inference technique propagates rewards on the graph from state-action pairs with rewards to state-action pairs without rewards and will converge to a unique fixed point after a few iterations.

We remark that TRAIN is not a naïve application of the LPA technique but a novel scalable method of learning propagation graphs that integrates multiple influence reward factors to edge weights. The graph sufficiently leverages various relationship information between nodes, which can make reward inference

more accurate. This has not been considered or evaluated in the context of offline RL reward learning. We also prove that the transductive inferred reward has a fixed point and at least can converge to a local optimum.

Our experiments demonstrate that the state-action pairs labeled by TRAIN significantly improve the offline reinforcement learning method when learning policy with limited reward annotations on complex locomotion and robotic manipulation tasks from DeepMind Control Suite [22] and Meta-World [23]. In particular, our method inherits the smooth characteristics of the LPA method [24], which can make the state-action pairs with smooth rewards and further make the process of offline RL algorithm learning policy more stable.

II. RELATED WORK

a) *Offline RL:* The offline reinforcement learning problem, which enables learning policies from the logged data instead of collecting it online, can be defined as a data-driven formulation of the reinforcement learning problem [1], [2], [3]. It is a promising approach for many real-world applications. Offline RL is an active area of research and many algorithms have been proposed recently, e.g., BCQ [25], MARWIL [26], BAIL [27], ABM [28], AWR [29], CRR [30], F-BRC [31]. In this paper, we adopt CRR as our backbone algorithm due to its efficiency and simplicity.

b) *Reward learning:* It is possible to learn the reward signal even when it is not constantly available in the environment. The reward can be learned if demonstrations are provided either directly with inverse RL [32], [33] or indirectly with generative adversarial imitation learning (GAIL) [34]. The end goal [35], [36] or reward values [10] for a subset of state-action pairs can be known, in which case reward functions can be learned by supervised learning. A significant instance of learning via limited reward supervision [10] is studied in some works. Rewards are commonly learned for online RL [37]. While learning from built or pre-trained state representations [38], [35], [39], [40], [41], [42], [43], [44] has achieved a lot of success, learning directly from pixel input is known to be difficult [45] and the quantity of supervision needed may become a bottleneck [10]. Unlike many other reward learning

approaches for offline RL, we focus on learning rewards with multi-factors that influenced rewards from limited annotations.

c) *Transduction*: The setting of transductive inference was first introduced by Vapnik [46]. Transductive Support Vector Machines (TSVMs) [47] is a margin-based categorization technique that reduces test set mistakes. Particularly for short training sets, it demonstrates considerable advantages over inductive techniques. Another classification of transduction methods involves graph-based methods [14], [16], [18], [48], [49]. Labels are transferred from labelled to unlabelled data instances through a process called label propagation, which is driven by the weighted graph. In prior works, the graph construction is done on a pre-defined feature space using only a single influence factor between nodes so that it is not possible to learn multi-factors influenced graph edge weights.

III. PROBLEM FORMULATION

The key to the TRAIN method is the prior assumption of consistency, which means: (1) nearby states and actions are likely to have similar or the same reward, and (2) state-action pairs on the same structure (typically referred to as a cluster or a manifold) are likely to have the similar or the same reward. This argument is akin to semi-supervised learning problems that in [50], [51], [52], [16], [53], [24], [54] and often called the *cluster assumption* [16], [52]. Orthodox supervised learning algorithms, such as k -NN, in general, depend only on the first assumption of local consistency [16], that is, k -NN makes every data point be similar to data points in its local neighborhood. Our method leverages the relation information between states and actions to formalize the intrinsic structure revealed by state-action pairs with reward and state-action pairs without reward and construct a reward inference function.

We assume that the training samples (both with reward and without reward) are given as $D = [(s_1, a_1), \dots, (s_Z, a_Z)]$, where (s_i, a_i) denotes the state-action pair, and D has Z pairs. Given this, let D_L denote the labelled state-action pair set of D with v pairs, and D_U denote the unlabelled state-action pair set of D with g pairs, that is, $D_L = [(s_1^L, a_1^L), \dots, (s_{Z_L}^L, a_{Z_L}^L)]$, $D_U = [(s_1^U, a_1^U), \dots, (s_{Z_U}^U, a_{Z_U}^U)]$, s.t., $Z_L + Z_U = Z$.

The Z rewards are denoted by $R = [r_1, \dots, r_Z]$, we split the reward set R into 2-sub-block, $R_L = [r_1^L, \dots, r_{Z_L}^L]$ denotes the subset of known rewards and $R_U = [r_1^U, \dots, r_{Z_U}^U]$ denotes the subset of unknown rewards. Suppose that we are given a small set D_L of the state-action pairs with reward. The rest of the state-action pairs $D_U = D \setminus D_L$ are without reward. TRAIN utilizes all samples and known rewards to learn a reward propagation graph and infer rewards for state-action pairs that are without reward.

IV. METHODOLOGY

A. Overview

We take advantage of the property of the Markov Decision Process (MDP) that the reward function on an MDP depends only on the current state and action. Therefore, we leverage the relationship between states and actions to learn the reward propagation graph and realize reward labeling for state-action pairs without rewards. As in offline Reinforcement Learning,

such state-action pairs are logged in a dataset D . In practice, D includes diverse state-action pairs produced for various tasks by scripted, random, or learned policies as well as human demonstrations [10].

B. Construct Reward Propagation Graph

The graph possesses the contextual properties of information propagation and the structure is characterized by connectivity, so that can model the interrelationships between entities. In a graph, edges connect nodes, and the information of nodes can be transmitted to other nodes through the connection relationship of edges. We need to use the limited state-action pairs with rewards to learn rewards for the state-action pairs without rewards. Therefore, we model state-action pairs as nodes and learn a reward propagation graph using the relationships between nodes, which transfers information from labelled reward nodes to unlabelled reward nodes.

a) *Graph construction*: For most reinforcement learning tasks, rewards are influenced by many factors. For instance, in task *Humanoid*, which is part of the DeepMind Control Suite [22], [55], the state consists of six parts: joint angles, the height of the torso, extremity positions, torso vertical orientation, the velocity of the center of mass, and the generalized velocity, and action also consists of several parts that represent the torques applied at the hinge joints. The reward is related to the upright state of the robot, the control operation of the actuator, and the moving speed, etc., which are closely related to each part of the above state and action, so we regard each part of the state and action as a factor that influences the reward.

Specifically, we denote $s_i = [s_{i_1}, s_{i_2}, s_{i_3}, \dots, s_{i_M}]$, where s_{i_m} is a sub-state with any given dimension, and s_i consists of M sub-states. Correspondingly, we denote $a_i = [a_{i_1}, a_{i_2}, a_{i_3}, \dots, a_{i_N}]$, where a_i is all of the actions performed given state s_i , and composed of N specific sub-actions of a_{i_n} .

We design a reward propagation graph construction method integrating multi-factors influencing the reward to tune the edge weights. To be specific, we employ a distance function $\rho_s(s_{i_m}, s_{j_m}), \forall i \neq j$ to measure the similarity of the sub-states, and also employ a distance function $\rho_a(a_{i_n}, a_{j_n}), \forall i \neq j$ to measure the similarity of the sub-actions, the two distance function could be Euclidean distance or others. Then, we define the multi-factor measure for state-action pairs as:

$$\ell(\mathcal{S}_i, \mathcal{S}_j) = [\rho_s(s_{i_1}, s_{j_1}), \dots, \rho_s(s_{i_M}, s_{j_M}), \rho_a(a_{i_1}, a_{j_1}), \dots, \rho_a(a_{i_N}, a_{j_N})] \in \mathbb{R}^{M+N}, \quad (1)$$

where $\mathcal{S}_i = (s_i, a_i)$ denotes the i -th state-action pair.

Further, we employ a reward shaping function f_Θ with the parameters Θ to tune multi-factors' contribution to the rewards and integrate them into the edge weight:

$$W_{ij} = \frac{\exp(-f_\Theta(\ell(\mathcal{S}_i, \mathcal{S}_j)))}{\sum_{j \neq i} \exp(-f_\Theta(\ell(\mathcal{S}_i, \mathcal{S}_j)))}, \forall i \neq j. \quad (2)$$

where W_{ij} is an element in matrix W , which is a $Z \times Z$ weight matrix. We let $W_{ii} = 0$ and we also have $\sum_j W_{ij} = 1, \forall i$. We define each state-action pair as a node in the graph and

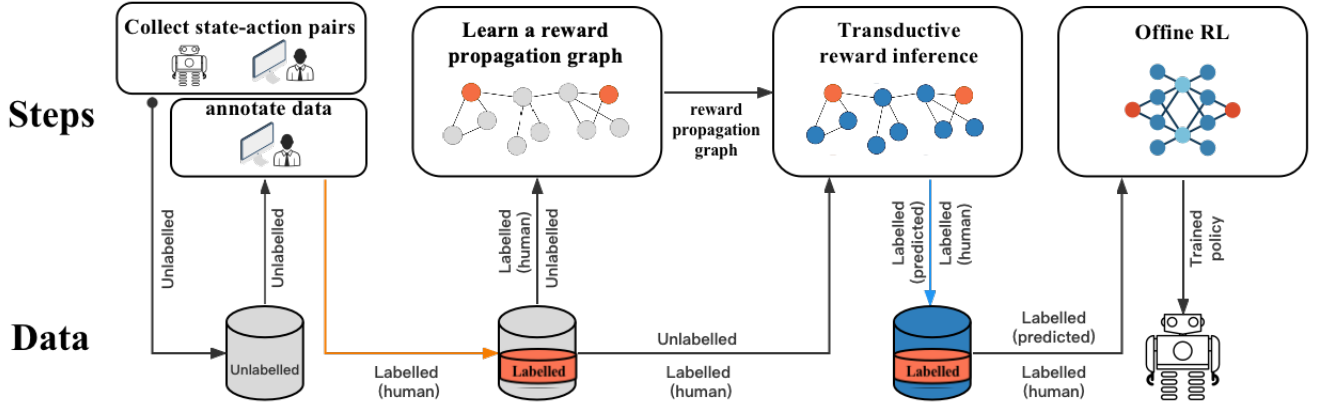


Fig. 2. TRAIN workflow: The process begins with the construction of a reward propagation graph using a pre-recorded dataset. Subsequently, this graph, in conjunction with state-action pairs that have rewards, is utilized to infer rewards for state-action pairs that lack rewards. In the final step, all state-action pairs, both with and without inferred rewards, are integrated into the offline reinforcement learning process.

define the weight between every two nodes in the graph, thus completing the construction of the reward propagation graph G with weight matrix W .

b) *Graph training*: In different tasks, the number of factors influencing reward is different, and the degree of influence of different factors on reward is also different. Therefore, we need to tune the weight of graph edges so that optimizing the function f_{Θ} to make the multi-factors efficiently integrate to rewards. Intuitively, for the state-action pair (s_i, a_i) , a larger edge weight W_{ij} means that state-action pair (s_j, a_j) will transfer more information to the reward for state-action pair (s_i, a_i) . Specifically, we use the relationship between labelled data to train f_{Θ} to make it suitable for the current task. We design a predicted reward ξ_l :

$$\xi_l = \sum_{k \neq l} W_{lk} r_k, \quad l, k \in [1, \dots, v], \quad (3)$$

where r_k is a label (reward) for a state-action pair (node). We use other labelled state-action pairs to predict the label of the current state-action pair (have a ground truth label) and then minimize the difference between the predicted label and the ground truth label.

Then, the goal of training the graph G is to optimize the parameters Θ for the function f_{Θ} , that is, minimize the difference between the predicted labels and their corresponding ground truth labels, the objective function $H(G)$ is given as:

$$\arg \min_{\Theta} \left\{ H(G) = \frac{1}{2Z_L} \sum_{l=1}^{Z_L} \|\xi_l - r_l\|^2 \right\}. \quad (4)$$

There does not exist a closed-form solution, and we use the gradient descent method to seek the solution, details are in the appendix A.

It should be noted that: the unlabelled data are not included in Equation (4), since the number of the unlabelled data is often much larger than that of the labelled data, the term on the unlabelled data may dominate the objective function, which in turn may degrade the algorithmic performance.

C. Transductive Reward Inference

In Section IV-B, we constructed the graph and trained the weights of the graph edges. In this section, we propagate reward-related information on the graph to infer the rewards for unlabelled state-action pairs based on the rewards of other state-action pairs.

We separate the weights associated with nodes without rewards from the weight matrix W of graph G formed by Equation (2), and represent them as two submatrices W_{UL} and W_{UU} . W_{UL} represents the weights between nodes with rewards and nodes without rewards, and W_{UU} represents the weights between nodes without rewards. We split the reward set R into two sub-blocks, R_L denotes the subset of known rewards and R_U denotes the subset of unknown rewards.

The inference of rewards for unlabelled nodes requires considering the information transfer between labelled and unlabelled nodes, we use $W_{UL}R_L$ for this calculation, while also taking into account the relationships between unlabeled nodes themselves, computed using $W_{UU}R_U$. Since unknown rewards R_U are a variable to be learned, we provide an iterative computation formula by:

$$R_U \leftarrow W_{UU}R_U + W_{UL}R_L. \quad (5)$$

After t -th iterations, we obtain the following formula:

$$R_U^t \leftarrow W_{UU}^t R_U^0 + (W_{UU}^{t-1} + \dots + W_{UU} + 1)W_{UL}R_L. \quad (6)$$

The detailed derivation process is in Appendix B. Based on the weights calculated by Equation (2), the values in W_{UU} are all less than 1. Therefore, as t approaches infinity, W_{UU}^t tends to infinitesimal values, leading $W_{UU}^t R_U^0$ converges to 0. Meanwhile, $(W_{UU}^{t-1} + \dots + W_{UU} + 1)$ forms a geometric series, and after applying the formula for the sum of a geometric series, we obtain the solution:

$$R_U = (I - W_{UU})^{(-1)} W_{UL} R_L, \quad (7)$$

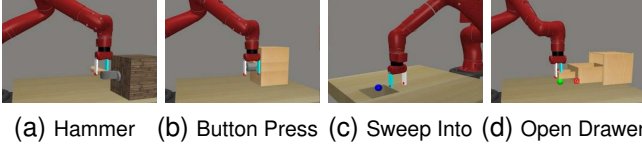


Fig. 3. Meta-World is a set of robotic manipulation tasks.

which is a *fixed point*, and I is the identity matrix [14], [16]. TRAIN converges to a *fixed point* means that the reward inference error is within a certain range.

D. Policy Learning

We remark that TRAIN can be combined with any offline RL algorithm by learning rewards for state-action pairs without reward. For learning a policy, we use a pre-recorded dataset D . Dataset D contains some state-action pairs with reward D_L , and most of the rest are state-action pairs without reward D_U . We use TRAIN to predict rewards for D_U as \tilde{D}_U , and then replace the part of D_U with the predicted rewards \tilde{D}_U to form \tilde{D} . We can then use \tilde{D} to train the policy. In this study, we employ Critic-Regularized Regression (CRR) [30], a simple and efficient offline reinforcement learning algorithm, to train offline reinforcement learning policies on the dataset with the predicted rewards.

V. EXPERIMENTS

A. Experiments setup

a) Environment and tasks: We conduct the experiments with a variety of complex robotic manipulation and locomotion tasks from Meta-World [23] and DeepMind Control Suite [22], [55], respectively. Many factors influence the reward function of these two series of tasks. Meta-World consists of a variety of manipulation tasks designed for learning diverse manipulation skills. The second environment is the DeepMind Control Suite, which contains many continuous control tasks involving locomotion and simple manipulation. To investigate the performance of TRAIN with a small amount of annotated state-action pairs. We conduct experiments on more than 40 tasks in the Meta-World environment, and we select four tasks (*Hammer*, *Button Press*, *Sweep Into*, *Open Drawer*) (see Fig. 3) of them to show their learning curves. We also choose five complex environments from DeepMind Control Suite: *Cheetah Run*, *Walker Walk*, *Fish Swim*, *Humanoid Run*, and *Cartpole Swingup* (see Fig. 4) to evaluate the performance of TRAIN in another environment different from the Meta-World, to verify whether the algorithm works only in one environment. On each task, we leverage different algorithms to predict the rewards for the same dataset and employ the CRR algorithm (except Behavior cloning) to perform policy learning on the dataset after predicting the rewards. The learned policies are used to evaluate the performance of TRAIN and other baselines. We report the results on all tasks of 5 random seeds, and results are shown in Section V-B.



Fig. 4. DeepMind Control Suite is a set of popular continuous control environments with tasks of varying difficulty, including locomotion and simple object manipulation.

b) Datasets: Given a set of logged state-action pairs (dataset D), we random extract a small subset of state-action pairs and leverage them as labelled data D_L , and others as D_U . The labels of D_L are the ground truth rewards. Meta-World domain has been used to evaluate online RL agents, we create an *ad hoc* dataset suitable for offline learning. To do so, we train Soft Actor-Critic [56] from full states on each of the tasks, and save the resulting replay buffer, which forms the dataset D . For DeepMind Control Suite, we use the open source RL Unplugged datasets [57] to form the dataset D for each task, the dataset also contains both successful and unsuccessful episodes. The total numbers of state-action pairs and the proportion of state-action pairs with ground truth rewards for each task are shown in Appendix C.

c) Baselines: Behavior cloning (BC) is a popular algorithm in the field of imitation learning and also an alternative way to learn a policy when the reward values are not available. BC agent does not require reward values as it attempts to directly imitate the demonstrated state-action pairs.

Time-guided reward (UDS) workflow, as outlined in [12], involves several key steps. Initially, it infers a reward function based on limited supervision, utilizing timestep-level annotations expressed as reward values on a subset of trajectories. Subsequently, it retroactively annotates all trajectories using the obtained reward function. Finally, the trajectories, now equipped with predicted rewards, are employed for offline reinforcement learning. Additionally, we integrated TGR with CRR (Critic Regularized Regression) [30] to learn policies as a baseline for our efforts. Specifically, TGR employs a two-step process for reward function inference. It starts by annotating demonstrated trajectories, assigning a flat zero synthetic reward to the unlabelled subset. The reward function is then trained using a loss function that jointly optimizes timestep-level annotations and synthetic flat labels. This comprehensive approach contributes to the effectiveness of TGR in the context of offline reinforcement learning. We also combined TGR with CRR [30] to learn policies.

Unlabeled data sharing (UDS) [13] addresses this scenario by treating the unlabeled dataset as if it has zero rewards, followed by the incorporation of reweighting techniques. This reweighting process is designed to adjust the distribution of interspersed zero-reward data. The primary objective is to synchronize the distribution of this external data with that of reward-containing data pertinent to the original task, thereby alleviating the bias introduced by inaccurate reward data. In particular, UDS initially assigns the minimum feasible reward (typically assumed to be 0) to all transitions within

the unlabeled data. Subsequently, these unlabeled transitions undergo reweighting, altering the distribution of unlabeled data to mitigate reward bias. This strategy contributes to the overall goal of enhancing the alignment between labeled and unlabeled data distributions in UDS. Finally, train offline reinforcement learning policies using the reweighted reward distribution dataset.

B. Experiments results

a) *Meta-world*: We show the evaluation results on more than 40 tasks in the Meta-World environment in Table I. Apart from the five tasks (*button-press*, *drawer-close*, *handle-press*, *reach*, *reach-wall*), the performance of the algorithm TRAIN exhibits greater superiority compared to others. This indicates that TRAIN achieves more accurate reward learning on these tasks. Additionally, due to its inherent smoothness, the learned rewards in TRAIN are smoother, leading to more stable policy performance. UDS emphasizes the need for high-quality labeled data. Since the data in our environment consists of SAC training data, and the labeled data is randomly selected, UDS performs well in relatively easy-to-learn tasks, specifically those with a higher proportion of high-quality data in the dataset, with particularly outstanding performance in the tasks of *button-press*, *drawer-close*, and *handle-press*. But, its performance is subpar in many other tasks.

Regarding the two tasks where the TGR algorithm outperforms others, we conducted a detailed analysis to identify the reasons. These tasks involve relatively simple action trajectories that are easily explored. The TGR algorithm annotates the demonstrated trajectories and assigns a flat zero synthetic reward to the unlabelled subset, which amplifies the rewards annotated as one along the action trajectories, encouraging the policy to learn these trajectories more actively. Therefore, TGR achieves better performance on such tasks. However, in other relatively complex tasks where the action trajectories for task completion are diverse, the method fails to provide accurate rewards for some procedural actions, resulting in mediocre policy performance. On the other hand, the poor performance of the Behavioral Cloning (BC) algorithm in many tasks can be attributed to its reliance on training with the entire dataset. The dataset comprises both successful and unsuccessful episodes, causing BC to be significantly affected by data quality. In tasks with relatively simple actions, algorithms that collect data can quickly learn the action trajectories for task completion, leading to a higher proportion of high-quality data in the dataset and thus better performance of BC. Conversely, in relatively complex tasks, data collection algorithms require a longer exploration process to learn the action trajectories for task completion, resulting in a lower proportion of high-quality data and consequently poor performance of BC.

We select four tasks of the Meta-World (*Hammer*, *Button Press*, *Sweep Into*, *Open Drawer*) to show their learning curves as measured on the success rate, as shown in Fig. 5. TRAIN outperforms the baselines on all four tasks, showing that TRAIN is well suited to make effective use of the unlabelled, mixed quality, state-action pairs. In the two tasks of Hammer and Sweep Into, TRAIN has always shown a

greater performance advantage compared to other baselines. In the two tasks of Button Press and Open Drawer, in the early stage of training, the performance of the three algorithms is equivalent, and the follow-up TRAIN gradually stands out. Especially in the Open Drawer task, a greater performance advantage has been achieved, while in the Button Press task, the training process of other baselines fluctuates greatly, and TRAIN has less fluctuation and achieves better performance. The conclusions drawn from the results in Fig. 5 are consistent with the conclusions drawn from the results in Table I. Italic numbers indicate the highest average return for each task, bold numbers indicate the statistically significant highest average return for each task, in which the average return is the highest, and there is not a clear overlap in the standard deviation among the baselines. TRAIN has an excellent performance from the aspect of the success rate demonstrating that TRAIN can effectively label rewards for state-action pairs without rewards, and the smoothness of the algorithm can make the labelled data also have smooth characteristics. The policies trained using these data have more stable performance.

b) *DeepMind Control Suite*: We show the learning curves of the five DeepMind Control Suite tasks (*Cheetah Run*, *Walker Walk*, *Fish Swim*, *Humanoid*, *Cartpole Swingup*) in Fig. 6. Our method TRAIN achieves better performance than baselines in five tasks. It has achieved a great performance advantage in the Walker Walk task, and also performed well in the Fish Swim task. The Cheetah Run and Cartpole Swingup tasks, also showed a certain performance advantage compared to TGR, although the advantage is not very large, it can still reflect the ability of the TRAIN algorithm. In the Humanoid task, TRAIN, UDS, and TGR are evenly matched during the training process, but the final performance of TRAIN is still better than other baselines, reflecting the stability of the state-action pairs with rewards provided by the TRAIN algorithm.

The action spaces of these five tasks are continuous, and the reward is also continuous. It is difficult to give a clear boundary to distinguish good actions and bad actions. Therefore, the performance of TRAIN and baselines are both very steady. However, the TRAIN algorithm has smooth characteristics, which can make the labelled data also have smooth characteristics. Using these state-action pairs with smooth rewards makes the process of offline RL algorithm learning policy more stable. Since the TGR algorithm annotates the demonstrated trajectories and assigns a flat zero synthetic reward to the unlabelled subset, it shows a large shock in the process of learning some tasks. UDS emphasizes the need for high-quality labeled data, resulting in slightly poorer performance. BC performed the worst among the five tasks, and hardly worked in the two tasks of Fish Swim and Cheetah Run. Because BC uses a complete data set for training, it cannot distinguish the quality of the data, and cannot obtain a policy with excellent performance.

C. Ablation study

We conducted a comprehensive set of ablation studies aimed at thoroughly evaluating the effectiveness of our reward shaping function, denoted as f_{Θ} . These experiments were meticulously

TABLE I

EVALUATION RETURNS ON MORE THAN 40 META-WORLD TASKS. THE AVERAGE \pm STANDARD DEVIATION IS SHOWN FOR FIVE RANDOM SEEDS.

| Tasks | BC | TGR | UDS | TRAIN |
|---------------------------|-------------------|-------------------|------------------|------------------------------------|
| basketball | 3019 \pm 439.6 | 978 \pm 122.7 | 3661 \pm 406.9 | 4165 \pm 315.9 |
| box-close | 1081 \pm 106.4 | 1568 \pm 119.8 | 1371 \pm 134.5 | 3897 \pm 412.3 |
| button-press | 1911 \pm 356 | 3301 \pm 291 | 3508 \pm 213.4 | 3435 \pm 106.4 |
| button-press-topdown | 3190 \pm 310.7 | 3401 \pm 415.7 | 3496 \pm 229.2 | 3587 \pm 75.4 |
| button-press-topdown-wall | 1892 \pm 50.2 | 2085 \pm 61.6 | 2069 \pm 48.7 | 2115 \pm 70.4 |
| coffee-button | 3531 \pm 710.6 | 3631 \pm 610.8 | 3923 \pm 352.4 | 4128 \pm 210.9 |
| coffee-pull | 517 \pm 16.3 | 372 \pm 11.5 | 314.2 \pm 7.9 | 637 \pm 35.2 |
| dial-turn | 1871 \pm 262.7 | 4217 \pm 395.4 | 4236 \pm 162.1 | 4428 \pm 185.9 |
| disassemble | 215 \pm 10.9 | 217 \pm 18.1 | 239.7 \pm 21.5 | 889 \pm 10.5 |
| door-close | 3862 \pm 167.1 | 4328 \pm 212.0 | 4451 \pm 184.2 | 4512 \pm 217.3 |
| door-lock | 3156 \pm 306.9 | 3536 \pm 285.1 | 3312 \pm 182.8 | 3753 \pm 195.2 |
| door-open | 1082 \pm 46.7 | 3985 \pm 306.9 | 1949 \pm 66.1 | 4451 \pm 197.1 |
| door-unlock | 1947 \pm 216.1 | 4011 \pm 75.3 | 2052 \pm 101.6 | 4189 \pm 118.9 |
| drawer-close | 4697 \pm 64.3 | 4839 \pm 102.1 | 4881 \pm 79.8 | 4797 \pm 20.3 |
| drawer-open | 1769 \pm 247 | 2890 \pm 86 | 1895 \pm 40.1 | 4466 \pm 41.3 |
| faucet-close | 4143 \pm 170.6 | 4687 \pm 821.6 | 4338 \pm 102.1 | 4712 \pm 147.1 |
| faucet-open | 3660 \pm 316.4 | 4702 \pm 1503.5 | 4671 \pm 361.8 | 4715 \pm 361.3 |
| hammer | 2205 \pm 268 | 3898 \pm 163 | 2692 \pm 101.5 | 4532 \pm 95.1 |
| hand-insert | 56 \pm 16.1 | 443 \pm 8.4 | 409 \pm 10.8 | 4016 \pm 598.6 |
| handle-press | 4598 \pm 137.9 | 4522 \pm 136.4 | 4651 \pm 82.4 | 4618 \pm 102.8 |
| handle-press-side | 4241 \pm 1353.4 | 4764 \pm 243.7 | 4734 \pm 185.2 | 4785 \pm 458.1 |
| handle-pull | 3892 \pm 986.8 | 4348 \pm 894.1 | 4138 \pm 147.6 | 4592 \pm 125.7 |
| handle-pull-side | 3678 \pm 1006.2 | 4095 \pm 572.6 | 3958 \pm 114.9 | 4551 \pm 92.8 |
| lever-pull | 3864 \pm 190.8 | 4184 \pm 175.1 | 4008 \pm 81.7 | 4307 \pm 135.7 |
| pick-out-of-hole | 11 \pm 0.4 | 209 \pm 3.5 | 117 \pm 12.2 | 1035 \pm 234.9 |
| pick-place | 1879 \pm 411.6 | 2975 \pm 495.6 | 3228 \pm 283.2 | 4106 \pm 589.4 |
| plate-slide | 3984 \pm 101.7 | 3674 \pm 748.3 | 4064 \pm 151.8 | 4459 \pm 171.4 |
| plate-slide-back | 3017 \pm 331.6 | 3158 \pm 958.4 | 3089 \pm 163.1 | 4658 \pm 165.3 |
| plate-slide-back-side | 4087 \pm 887.5 | 4678 \pm 172.6 | 4703 \pm 136.8 | 4734 \pm 198.4 |
| plate-slide-side | 2698 \pm 538.8 | 3002 \pm 365.3 | 2928 \pm 289.1 | 3010 \pm 429.5 |
| push | 1983 \pm 381.9 | 2097 \pm 261.4 | 2248 \pm 175.2 | 4268 \pm 210.7 |
| push-back | 9 \pm 0.4 | 137 \pm 1.5 | 79 \pm 8.7 | 201.3 \pm 21.7 |
| push-wall | 3642 \pm 597.8 | 4347 \pm 187.4 | 4182 \pm 155.8 | 4501 \pm 204.6 |
| reach | 3209 \pm 397.2 | 4761 \pm 476.6 | 4581 \pm 181.2 | 4668 \pm 215.6 |
| reach-wall | 4626 \pm 91.8 | 4816 \pm 51.1 | 4672 \pm 30.4 | 4810 \pm 36.3 |
| stick-pull | 592 \pm 10.8 | 442 \pm 7.2 | 408 \pm 7.8 | 4128 \pm 121.5 |
| stick-push | 362 \pm 16.2 | 887 \pm 5.3 | 1065 \pm 21.7 | 2745 \pm 514.3 |
| sweep | 879 \pm 145.6 | 3214 \pm 412.7 | 3708 \pm 237.1 | 4106 \pm 312.7 |
| sweep-into | 962 \pm 137 | 1838 \pm 149 | 2115 \pm 176.5 | 2257 \pm 323.9 |
| window-close | 3846 \pm 98.3 | 4104 \pm 106.1 | 4354 \pm 86.4 | 4458 \pm 88.4 |
| window-open | 3217 \pm 193.2 | 2897 \pm 954.5 | 3141 \pm 105.5 | 3829 \pm 208.4 |

designed and carried out across a diverse set of environments, including four Meta-World environments and five DeepMind Control Suite environments.

In our investigation, we delved into the intricate interplay of various factors that influence the rewards associated with nine distinct tasks. To provide a detailed assessment, we employed four distinct composition methods, each shedding light on the role of factors related to both states and actions:

- (1) Method 1: In this approach, both states and actions underwent decomposition into multiple factors, allowing us to scrutinize the combined impact of these nuanced elements.
- (2) Method 2: Here, we selectively decomposed states into multiple factors while treating actions as a unified entity. This method offered insights into how states, in isolation, contribute to the shaping of rewards.
- (3) Method 3: Conversely, we kept states as a single, undivided factor but decomposed actions into multiple components. This experiment assessed the significance of dissecting actions in the reward-shaping process.

- (4) Method 4: As a contrast, we simplified the scenario by considering both states and actions as single, undifferentiated factors. This method served as a baseline for evaluating the performance of more complex factorization approaches.

The experimental results are shown in Table II. Italic numbers indicate the highest average return for each task. Bold numbers indicate the statistically significant highest average return for each task, in which the average return is the highest, and there is not a clear overlap in the standard deviation among the baselines.

The compelling results that emerged from our extensive experimentation affirmed the superiority of Method 1, where both states and actions were decomposed into multiple factors. This approach consistently demonstrated the most favorable outcomes across the range of tasks we examined.

On the other hand, Method 2, which decomposed states while treating actions as single entities, produced results that, while respectable, fell short of the peak performance achieved by Method 1.

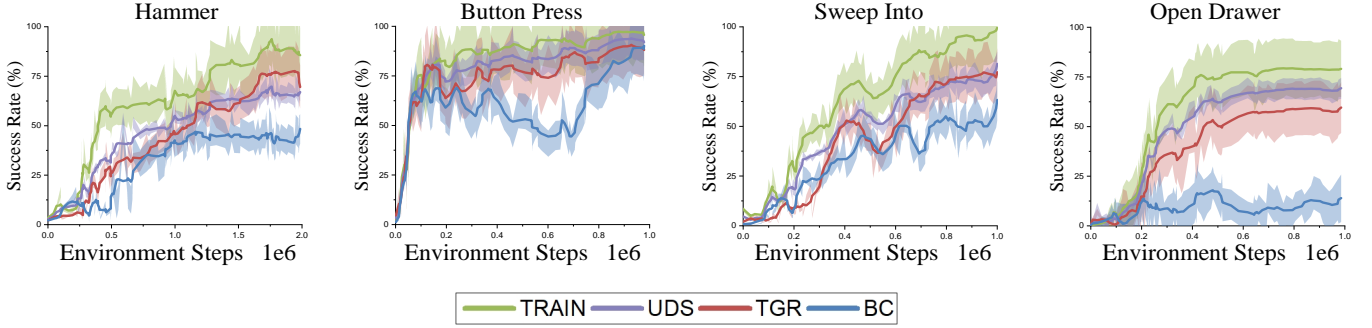


Fig. 5. Learning curves on the four Meta-World tasks as measured on the success rate. The solid line and shaded regions represent the mean and standard deviation, respectively, across five seeds.

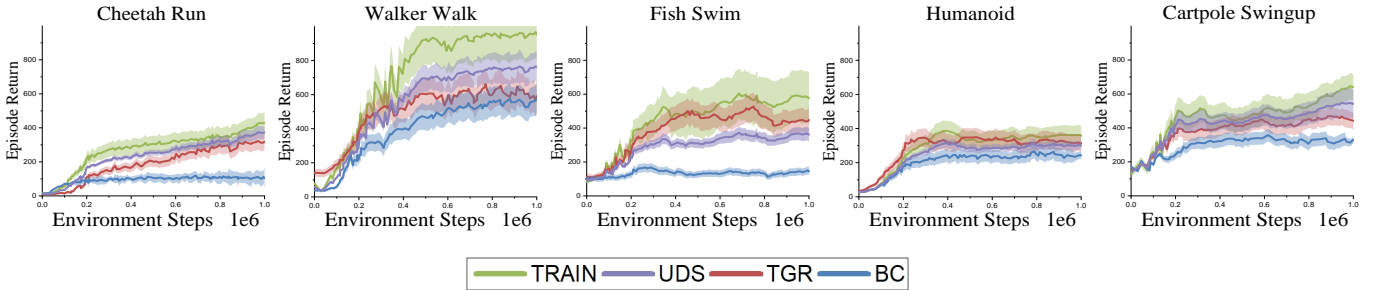


Fig. 6. Learning curves on the five DM Control tasks as measured on the episode return. The solid line and shaded regions represent the mean and standard deviation, respectively, across five seeds.

TABLE II

EVALUATION RETURNS ON FOUR DIFFERENT COMPOSITION METHODS FOR THE MULTIPLE FACTORS THAT INFLUENCE THE REWARDS. THE AVERAGE \pm STANDARD DEVIATION IS SHOWN FOR FIVE RANDOM SEEDS.

| Tasks | Method 1 | Method 2 | Method 3 | Method 4 |
|------------------|---------------------------------|----------------|----------------|----------------|
| Hammer | 4532 \pm 95 | 3158 \pm 242 | 2185 \pm 262 | 1034 \pm 147 |
| Sweep Into | 2257 \pm 324 | 1971 \pm 243 | 1734 \pm 276 | 665 \pm 185 |
| Button Press | 3435 \pm 106 | 3145 \pm 227 | 2576 \pm 85 | 1089 \pm 290 |
| Open Drawer | 4466 \pm 41 | 2998 \pm 64 | 2514 \pm 54 | 1727 \pm 75 |
| Cheetah Run | 430 \pm 55 | 361 \pm 138 | 255 \pm 126 | 183 \pm 74 |
| Walker Walk | 950 \pm 155 | 714 \pm 83 | 463 \pm 76 | 262 \pm 38 |
| Fish Swim | 576 \pm 155 | 453 \pm 26 | 296 \pm 89 | 198 \pm 29 |
| Humanoid Run | 359 \pm 57 | 201 \pm 31 | 154 \pm 38 | 26 \pm 4 |
| Cartpole Swingup | 642 \pm 68 | 441 \pm 29 | 349 \pm 18 | 208 \pm 17 |

A noteworthy revelation emerged when we explored Method 4, where both states and actions were considered as single factors. This approach exhibited a stark drop in performance, and in some slightly complex environments, it led to outright failures. This finding underscores the critical importance of factorization and highlights the perils of oversimplifying the reward-shaping process.

In light of these insights, we conclude that decomposing both states and actions into multiple factors and seamlessly integrating them using f_{Θ} stands as the most effective strategy. This sophisticated approach enables a finer level of granularity in reward learning and significantly enhances the overall efficacy of policies trained on datasets subjected to such comprehensive factorization.

1) *Image-based experiments:* Our novel approach, TRAIN, showcases a remarkable degree of adaptability that extends beyond conventional full-state tasks, seamlessly accommodating image-based tasks with equal prowess. In our quest to assess TRAIN’s performance in the realm of image-based tasks, we ingeniously conditioned the environment’s output to generate images, thus opening up exciting possibilities for visual-based learning scenarios.

Furthermore, we integrated a widely endorsed strategy employed in diverse task domains, wherein we treated multiple frames as a single time-step state. These frames underwent a meticulous process of decomposition into interdependent frames, and each frame was subsequently subjected to further dissection into RGB channels, effectively treating each single image as an individual factor.

Our experimentation with TRAIN spanned a diverse set of environments, encompassing four distinct Meta-World environments and an additional five environments sourced from the esteemed DeepMind Control Suite. The breadth of this evaluation allowed us to gain comprehensive insights into TRAIN’s capabilities in a variety of settings. The results are shown in Fig. 7.

The experimental results that emerged from these rigorous trials underscored TRAIN’s robust performance in image-based experiments. This underscores the effectiveness of our approach in seamlessly integrating multiple images within a single time step, each image serving as a distinct factor. This multi-faceted approach capitalizes on the richness of information inherent in each image, ultimately enhancing the depth and quality of

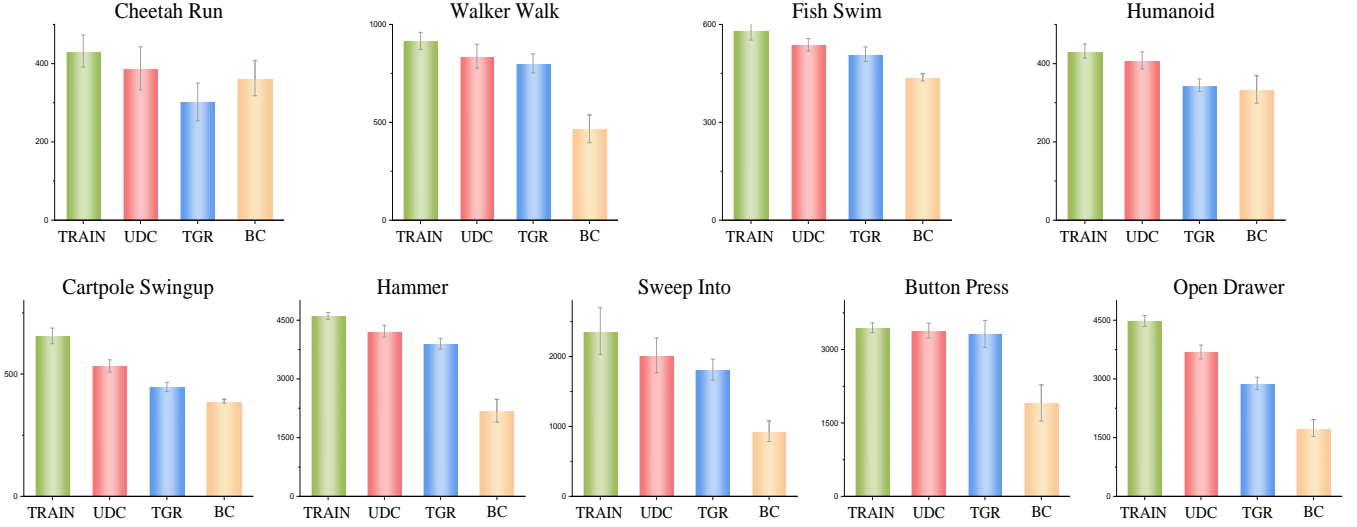


Fig. 7. Evaluation returns on the nine image-based tasks. The vertical lines depict the standard deviation across five random seeds of each experiment.

the learning process. TRAIN’s ability to harness the unique information contained within each image not only expands its versatility but also positions it as a promising candidate for a wide array of image-driven applications in the realm of artificial intelligence.

D. Accurate of predicted labels on different labelled data proportion

To rigorously assess the predictive accuracy of our innovative approach, TRAIN, across varying ratios of labeled data, we embarked on a comprehensive evaluation campaign. Our experiments spanned a diverse range of environments, encompassing four challenging Meta-World scenarios and an additional five environments sourced from the prestigious DeepMind Control Suite.

In Fig. 8, we present a vivid representation of our findings, utilizing the mean squared error (MSE) as our primary evaluation metric. This heatmap graphically depicts the relationship between multiple tasks (on the horizontal axis) and the ratio of reward-labeled data in the dataset (on the vertical axis). Each value in the figure reflects the MSE associated with a specific task under the corresponding labeled data ratio. To ensure the robustness of our findings, we partitioned the dataset into multiple batches, with the calculated result representing the average MSE value across these batches.

The compelling insights derived from our experiments reveal a clear trend: as the ratio of reward-labeled data in the dataset increases, the corresponding MSE values decrease, indicating a higher degree of predictive accuracy. Conversely, a lower ratio of labeled reward data in the dataset is associated with higher MSE values, signifying a relatively lower predictive accuracy. Furthermore, our observations indicate that tasks characterized by higher-dimensional states and actions tend to exhibit elevated MSE values, suggesting that predictive challenges are more pronounced in these complex settings.

These findings offer valuable insights into the performance of TRAIN across a spectrum of labeled data ratios and task

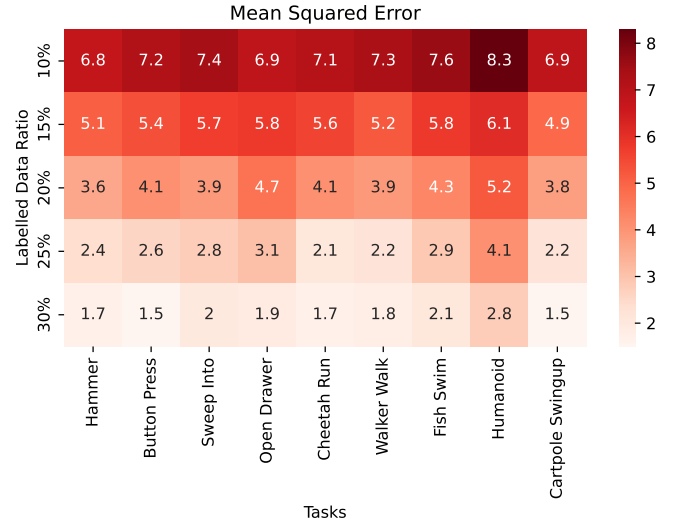


Fig. 8. The accuracy between predicted labels and ground truth labels of TRAIN under different labelled data ratios on four Meta-World and five DeepMind Control Suite environments, respectively. The evaluation metric is the mean squared error (MSE).

complexities, shedding light on its capabilities and areas for potential refinement. Such detailed evaluations are instrumental in understanding the nuances of our approach’s predictive accuracy and provide a roadmap for its application in real-world scenarios across various domains.

E. Accurate of predicted labels on different norms

To assess the accuracy of our proposed method, TRAIN, in relation to different norms, we conducted experiments using four Meta-World and five DeepMind Control Suite environments. Fig. 8 illustrates the results, utilizing the mean squared error (MSE) as the evaluation metric.

It’s important to note that the 1.5 norm and the 2.5 norm were introduced purely for experimentation purposes and

lack specific physical interpretations. These two norms were included to investigate the impact of norm selection on our method.

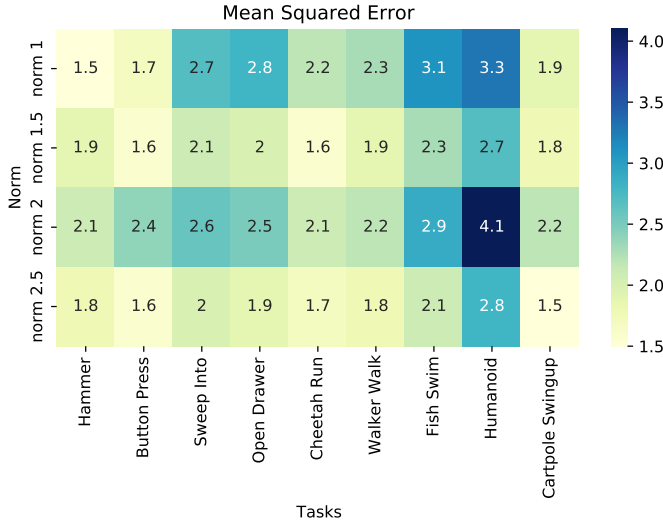


Fig. 9. The accuracy between predicted labels and ground truth labels of TRAIN under different norms on four Meta-World and five DeepMind Control Suite environments, respectively. The evaluation metric is the mean squared error (MSE).

In the heatmap of the experimental outcomes, the horizontal axis represents various tasks, the vertical axis corresponds to different norms, and the values within the figure indicate the MSE for each task under a specific norm. The dataset was partitioned into multiple batches, and the calculated result represents the average MSE across these batches.

From the experimental results, it is evident that different norms have minimal influence on the MSE, indicating that our method TRAIN is not sensitive to the choice of norm, underscoring its robustness in various scenarios.

VI. CONCLUSION

In conclusion, our research proposes the TRAIN method to address a critical challenge in offline reinforcement learning by developing a reward inference method that leverages a constrained number of human reward annotations to estimate rewards for unlabelled data. TRAIN models MDPs as a graph and leverage the contextual properties of information propagation of the graph structure to construct a reward propagation graph that incorporates various influential factors, facilitating transductive reward inference. We have shown the existence of a fixed point during the iterative inference process, and our method converges at least to a local optimum. Empirical evaluations on locomotion and robotic manipulation tasks demonstrate the effectiveness of TRAIN, especially when dealing with limited reward annotations. This work has significant implications for practical scenarios where reward functions are challenging to access.

REFERENCES

[1] S. Lange, T. Gabel, and M. Riedmiller, “Batch reinforcement learning,” in *Reinforcement learning*. Springer, 2012, pp. 45–73.

[2] S. Levine, A. Kumar, G. Tucker, and J. Fu, “Offline reinforcement learning: Tutorial, review, and perspectives on open problems,” *arXiv preprint arXiv:2005.01643*, 2020.

[3] R. F. Prudencio, M. R. Maximo, and E. L. Colombari, “A survey on offline reinforcement learning: Taxonomy, review, and open problems,” *IEEE Transactions on Neural Networks and Learning Systems*, 2023.

[4] S. Cabi, S. G. Colmenarejo, A. Novikov, K. Konyushkova, S. Reed, R. Jeong, K. Zolna, Y. Aytar, D. Budden, M. Vecerik *et al.*, “Scaling data-driven robotics with reward sketching and batch reinforcement learning,” *arXiv preprint arXiv:1909.12200*, 2019.

[5] S. Dasari, F. Ebert, S. Tian, S. Nair, B. Bucher, K. Schmeckpeper, S. Singh, S. Levine, and C. Finn, “Robonet: Large-scale multi-robot learning,” in *Conference on Robot Learning*. PMLR, 2020, pp. 885–897.

[6] F. Yu, W. Xian, Y. Chen, F. Liu, M. Liao, V. Madhavan, and T. Darrell, “Bddl00k: A diverse driving video database with scalable annotation tooling,” *arXiv preprint arXiv:1805.04687*, vol. 2, no. 5, p. 6, 2018.

[7] A. Strehl, J. Langford, L. Li, and S. M. Kakade, “Learning from logged implicit exploration data,” *Advances in neural information processing systems*, vol. 23, 2010.

[8] L. Bottou, J. Peters, J. Quiñonero-Candela, D. X. Charles, D. M. Chickering, E. Portugaly, D. Ray, P. Simard, and E. Snelson, “Counterfactual reasoning and learning systems: The example of computational advertising,” *Journal of Machine Learning Research*, vol. 14, no. 11, 2013.

[9] S. M. Shortreed, E. Laber, D. J. Lizotte, T. S. Stroup, J. Pineau, and S. A. Murphy, “Informing sequential clinical decision-making through reinforcement learning: an empirical study,” *Machine learning*, vol. 84, no. 1, pp. 109–136, 2011.

[10] S. Cabi, S. G. Colmenarejo, A. Novikov, K. Konyushkova, S. Reed, R. Jeong, K. Zolna, Y. Aytar, D. Budden, M. Vecerik *et al.*, “Scaling data-driven robotics with reward sketching and batch reinforcement learning,” in *Robotics: Science and Systems Conference*, 2020.

[11] K. Zolna, A. Novikov, K. Konyushkova, C. Gulcehre, Z. Wang, Y. Aytar, M. Denil, N. de Freitas, and S. Reed, “Offline learning from demonstrations and unlabeled experience,” *arXiv preprint arXiv:2011.13885*, 2020.

[12] K. Konyushkova, K. Zolna, Y. Aytar, A. Novikov, S. Reed, S. Cabi, and N. de Freitas, “Semi-supervised reward learning for offline reinforcement learning,” *arXiv preprint arXiv:2012.06899*, 2020.

[13] T. Yu, A. Kumar, Y. Chebotar, K. Hausman, C. Finn, and S. Levine, “How to leverage unlabeled data in offline reinforcement learning,” in *International Conference on Machine Learning*. PMLR, 2022, pp. 25 611–25 635.

[14] X. Zhu and Z. Ghahramani, “Learning from labeled and unlabeled data with label propagation,” *ProQuest number: information to all users*, 2002.

[15] X. Zhu, *Semi-supervised learning with graphs*. Carnegie Mellon University, 2005.

[16] D. Zhou, O. Bousquet, T. Lal, J. Weston, and B. Schölkopf, “Learning with local and global consistency,” *Advances in neural information processing systems*, vol. 16, 2003.

[17] X. Zhang and W. Lee, “Hyperparameter learning for graph based semi-supervised learning algorithms,” *Advances in neural information processing systems*, vol. 19, 2006.

[18] F. Wang and C. Zhang, “Label propagation through linear neighborhoods,” in *Proceedings of the 23rd international conference on Machine learning*, 2006, pp. 985–992.

[19] M. Karasuyama and H. Mamitsuka, “Manifold-based similarity adaptation for label propagation,” *Advances in neural information processing systems*, vol. 26, 2013.

[20] C. Gong, D. Tao, W. Liu, L. Liu, and J. Yang, “Label propagation via teaching-to-learn and learning-to-teach,” *IEEE transactions on neural networks and learning systems*, vol. 28, no. 6, pp. 1452–1465, 2016.

[21] Y. Liu, J. Lee, M. Park, S. Kim, E. Yang, S. J. Hwang, and Y. Yang, “Learning to propagate labels: Transductive propagation network for few-shot learning,” in *International Conference on Learning Representations*, 2019.

[22] Y. Tassa, Y. Doron, A. Muldal, T. Erez, Y. Li, D. d. L. Casas, D. Budden, A. Abdolmaleki, J. Merel, A. Lefrancq *et al.*, “Deepmind control suite,” *arXiv preprint arXiv:1801.00690*, 2018.

[23] T. Yu, D. Quillen, Z. He, R. Julian, K. Hausman, C. Finn, and S. Levine, “Meta-world: A benchmark and evaluation for multi-task and meta reinforcement learning,” in *Conference on robot learning*. PMLR, 2020, pp. 1094–1100.

[24] H. Wang and J. Leskovec, “Unifying graph convolutional neural networks and label propagation,” *arXiv preprint arXiv:2002.06755*, 2020.

- [25] S. Fujimoto, D. Meger, and D. Precup, "Off-policy deep reinforcement learning without exploration," in *International conference on machine learning*. PMLR, 2019, pp. 2052–2062.
- [26] Q. Wang, J. Xiong, L. Han, H. Liu, T. Zhang *et al.*, "Exponentially weighted imitation learning for batched historical data," *Advances in Neural Information Processing Systems*, vol. 31, 2018.
- [27] X. Chen, Z. Zhou, Z. Wang, C. Wang, Y. Wu, and K. Ross, "Bail: Best-action imitation learning for batch deep reinforcement learning," *Advances in Neural Information Processing Systems*, vol. 33, pp. 18 353–18 363, 2020.
- [28] N. Y. Siegel, J. T. Springenberg, F. Berkenkamp, A. Abdolmaleki, M. Neunert, T. Lampe, R. Hafner, N. Heess, and M. Riedmiller, "Keep doing what worked: Behavioral modelling priors for offline reinforcement learning," in *International Conference on Learning Representations*, 2020.
- [29] X. B. Peng, A. Kumar, G. Zhang, and S. Levine, "Advantage-weighted regression: Simple and scalable off-policy reinforcement learning," *arXiv preprint arXiv:1910.00177*, 2019.
- [30] Z. Wang, A. Novikov, K. Zolna, J. S. Merel, J. T. Springenberg, S. E. Reed, B. Shahriari, N. Siegel, C. Gulcehre, N. Heess *et al.*, "Critic regularized regression," *Advances in Neural Information Processing Systems*, vol. 33, pp. 7768–7778, 2020.
- [31] I. Kostrikov, R. Fergus, J. Tompson, and O. Nachum, "Offline reinforcement learning with fisher divergence critic regularization," in *International Conference on Machine Learning*. PMLR, 2021, pp. 5774–5783.
- [32] P. Abbeel and A. Y. Ng, "Apprenticeship learning via inverse reinforcement learning," in *Proceedings of the twenty-first international conference on Machine learning*, 2004, p. 1.
- [33] A. Y. Ng, S. Russell *et al.*, "Algorithms for inverse reinforcement learning," in *Icml*, vol. 1, 2000, p. 2.
- [34] J. Ho and S. Ermon, "Generative adversarial imitation learning," *Advances in neural information processing systems*, vol. 29, 2016.
- [35] A. Edwards, C. Isbell, and A. Takanishi, "Perceptual reward functions," *arXiv preprint arXiv:1608.03824*, 2016.
- [36] A. Singh, L. Yang, K. Hartikainen, C. Finn, and S. Levine, "End-to-end robotic reinforcement learning without reward engineering," *arXiv preprint arXiv:1904.07854*, 2019.
- [37] M. Klissarov and D. Precup, "Reward propagation using graph convolutional networks," *Advances in Neural Information Processing Systems*, vol. 33, pp. 12 895–12 908, 2020.
- [38] N. Baram, O. Anschel, I. Caspi, and S. Mannor, "End-to-end differentiable adversarial imitation learning," in *International Conference on Machine Learning*. PMLR, 2017, pp. 390–399.
- [39] C. Finn, S. Levine, and P. Abbeel, "Guided cost learning: Deep inverse optimal control via policy optimization," in *International conference on machine learning*. PMLR, 2016, pp. 49–58.
- [40] J. Fu, K. Luo, and S. Levine, "Learning robust rewards with adversarial inverse reinforcement learning," *arXiv preprint arXiv:1710.11248*, 2017.
- [41] Y. Li, J. Song, and S. Ermon, "Infogail: Interpretable imitation learning from visual demonstrations," *Advances in Neural Information Processing Systems*, vol. 30, 2017.
- [42] J. Merel, Y. Tassa, D. TB, S. Srinivasan, J. Lemmon, Z. Wang, G. Wayne, and N. Heess, "Learning human behaviors from motion capture by adversarial imitation," *arXiv preprint arXiv:1707.02201*, 2017.
- [43] P. Sermanet, K. Xu, and S. Levine, "Unsupervised perceptual rewards for imitation learning," *arXiv preprint arXiv:1612.06699*, 2016.
- [44] Y. Zhu, Z. Wang, J. Merel, A. Rusu, T. Erez, S. Cabi, S. Tunyasuvunakool, J. Kramár, R. Hadsell, N. de Freitas *et al.*, "Reinforcement and imitation learning for diverse visuomotor skills," *arXiv preprint arXiv:1802.09564*, 2018.
- [45] K. Zolna, S. Reed, A. Novikov, S. G. Colmenarejo, D. Budden, S. Cabi, M. Denil, N. de Freitas, and Z. Wang, "Task-relevant adversarial imitation learning," in *Conference on Robot Learning*. PMLR, 2021, pp. 247–263.
- [46] V. N. Vapnik, "An overview of statistical learning theory," *IEEE transactions on neural networks*, vol. 10, no. 5, pp. 988–999, 1999.
- [47] T. Joachims *et al.*, "Transductive inference for text classification using support vector machines," in *Icml*, vol. 99, 1999, pp. 200–209.
- [48] M. Rohrbach, S. Ebert, and B. Schiele, "Transfer learning in a transductive setting," *Advances in neural information processing systems*, vol. 26, 2013.
- [49] Y. Fu, T. M. Hospedales, T. Xiang, and S. Gong, "Transductive multi-view zero-shot learning," *IEEE transactions on pattern analysis and machine intelligence*, vol. 37, no. 11, pp. 2332–2345, 2015.
- [50] M. Belkin and P. Niyogi, "Semi-supervised learning on manifolds," *Machine Learning Journal*, vol. 1, 2002.
- [51] A. Blum and S. Chawla, "Learning from labeled and unlabeled data using graph mincuts," in *Proceedings of the Eighteenth International Conference on Machine Learning*, 2001, pp. 19–26.
- [52] O. Chapelle, J. Weston, and B. Schölkopf, "Cluster kernels for semi-supervised learning," *Advances in neural information processing systems*, vol. 15, 2002.
- [53] X. Zhu, Z. Ghahramani, and J. D. Lafferty, "Semi-supervised learning using gaussian fields and harmonic functions," in *Proceedings of the 20th International conference on Machine learning (ICML-03)*, 2003, pp. 912–919.
- [54] A. Iscen, G. Tolias, Y. Avrithis, and O. Chum, "Label propagation for deep semi-supervised learning," in *Proceedings of the IEEE/CVF Conference on Computer Vision and Pattern Recognition*, 2019, pp. 5070–5079.
- [55] S. Tunyasuvunakool, A. Muldal, Y. Doron, S. Liu, S. Bohez, J. Merel, T. Erez, T. Lillicrap, N. Heess, and Y. Tassa, "dm_control: Software and tasks for continuous control," *Software Impacts*, vol. 6, p. 100022, 2020.
- [56] T. Haarnoja, A. Zhou, P. Abbeel, and S. Levine, "Soft actor-critic: Off-policy maximum entropy deep reinforcement learning with a stochastic actor," in *International conference on machine learning*. PMLR, 2018, pp. 1861–1870.
- [57] C. Gulcehre, Z. Wang, A. Novikov, T. Le Paine, S. G. Colmenarejo, K. Zolna, R. Agarwal, J. Merel, D. Mankowitz, C. Paduraru *et al.*, "RL unplugged: Benchmarks for offline reinforcement learning," *arXiv preprint arXiv:2006.13888*, vol. 394, 2020.



Bohao Qu Bohao Qu is currently pursuing the Ph.D. degree with the School of Artificial Intelligence, Jilin University, Changchun, China. He is also a visiting student with the A*STAR Centre for Frontier AI Research, Singapore. Before that, he was an engineer of JD Mall Research, Beijing, China, from 2017 to 2019. His current research interests include deep reinforcement learning, machine learning, and hyperbolic (non-Euclidean) geometry.



Xiaofeng Cao received his Ph.D. degree at Australian Artificial Intelligence Institute, University of Technology Sydney, Australia, and was a visiting scholar at the Hong Kong University of Science and Technology. He is currently an Associate Professor at the School of Artificial Intelligence, Jilin University, China, and leading the Machine Perceptron Research Group with more than 20 members. He has more than 30 academic works published in IEEE T-PAMI, TNNLS, ICML, NeurIPS, ICLR, ECML, etc, and served as their PC members/reviewers. His research interests

include the PAC learning theory, agnostic learning algorithm, generalization analysis, and hyperbolic (non-Euclidean) geometry.



Qing Guo received his Ph.D. degree in computer application technology from the School of Computer Science and Technology, Tianjin University, China. He is currently a senior research scientist and principal investigator (PI) at the Center for Frontier AI Research (CFAR), A*STAR in Singapore. He is also an adjunct assistant professor at the National University of Singapore (NUS), and senior PC member of AAAI. Before that, he was a Wallenberg-NTU Presidential Postdoctoral Fellow with the Nanyang Technological University, Singapore. His research

interests include computer vision, AI security, and image processing. He is a member of IEEE.



Yi Chang is currently the Dean of the School of Artificial Intelligence, Jilin University, Changchun, China. He became a Chinese National Distinguished Professor in 2017 and the ACM Distinguished Scientist in 2018. Before joining academia, he was the Technical Vice President at Huawei Research America, in charge of knowledge graph, question answering, and vertical search projects. Before that, he was the Research Director of Yahoo Labs/Research, USA, from 2006 to 2016, in charge of search relevance of Yahoo's web search engine and vertical search

engines. He is the author of two books and more than 100 papers in top conferences or journals. His research interests include information retrieval, data mining, machine learning, natural language processing, and artificial intelligence.

Dr. Chang won the Best Paper Award on ACM KDD 2016 and ACM International WSDM Conference 2016. He has served as one of the Conference General Chair for ACM International WSDM Conference 2018 and International ACM SIGIR Conference on Research and Development in Information Retrieval 2020. He is an Associate Editor of IEEE Transactions on Knowledge and Data Engineering.



Ivor W. Tsang (Fellow IEEE) is currently the Director of the A*STAR Centre for Frontier AI Research, Singapore. He is also a Professor of artificial intelligence with the University of Technology Sydney, Ultimo, NSW, Australia, and the Research Director of the Australian Artificial Intelligence Institute. His research interests include transfer learning, deep generative models, learning with weakly supervision, Big Data analytics for data with extremely high dimensions in features, samples and labels.

In 2013, he was the recipient of the ARC Future Fellowship for his outstanding research on Big Data analytics and large-scale machine learning. In 2019, his JMLR paper Towards ultrahigh dimensional feature selection for Big Data was the recipient of the International Consortium of Chinese Mathematicians Best Paper Award. In 2020, he was recognized as the AI 2000 AAAI/IJCAI Most Influential Scholar in Australia for his outstanding contributions to the field between 2009 and 2019. Recently, he was conferred the IEEE Fellow for his outstanding contributions to large-scale machine learning and transfer learning. He serves as the Editorial Board for the JMLR, MLJ, JAIR, IEEE TPAMI, IEEE TAI, IEEE TBD, and IEEE TETCI. He serves/served as a AC or Senior AC for NeurIPS, ICML, AAAI and IJCAI, and the steering committee of ACML.



Chengqi Zhang Chengqi Zhang received a Ph.D. from the University of Queensland, Brisbane, Australia, in 1991 and a DSc (higher doctorate) from Deakin University, Geelong, Australia, in 2002. Since December 2001, he has been a Professor of Information Technology with the University of Technology Sydney (UTS), Australia, where he was Director of the UTS Priority Investment Research Centre for Quantum Computation and Intelligent Systems from 2008-2016. His research interests mainly focus on data mining and its applications. He was General

Co-Chair of KDD 2015 in Sydney, the Local Arrangements Chair of IJCAI-2017 in Melbourne, and a General Chair of IJCAI-2024 in Jeju Island, and is a Fellow of the Australian Computer Society and a Senior Member of the IEEE.

APPENDIX A GRADIENT

For the graph G , we design the training loss function $H(G)$ in Equation (4), there does not exist a closed-form solution, and we use the gradient descent method to seek the solution. The gradient with respect to Θ is given in Equation (8),

$$\begin{aligned}
\frac{\partial H}{\partial \Theta} &= -\frac{1}{Z_L} \sum_l (r_l - \xi_l) \frac{\partial \xi_l}{\partial \Theta} \\
&= -\frac{1}{Z_L} \sum_l (r_l - \xi_l) (-2\Theta) \\
&\quad \left\{ \left[\sum_{k \neq l} r_k \xi_{lk} (\rho_s(s_l, s_k) + \rho_a(a_l, a_k))^2 \right] \right. \\
&\quad \left. - \left[\sum_{k \neq l} r_k \xi_{lk} \right] \left[\sum_{k \neq l} \xi_{lk} (\rho_s(s_l, s_k) + \rho_a(a_l, a_k))^2 \right] \right\} \\
&= \frac{2\Theta}{Z_L} \sum_l (r_l - \xi_l) \left\{ \left[\sum_{k \neq l} r_k \xi_{lk} (\rho_s(s_l, s_k) + \rho_a(a_l, a_k))^2 \right] \right. \\
&\quad \left. - [\xi_l] \left[\sum_{k \neq l} \xi_{lk} (\rho_s(s_l, s_k) + \rho_a(a_l, a_k))^2 \right] \right\} \\
&= \frac{2\Theta}{Z_L} \sum_l (r_l - \xi_l) \left\{ \left[\sum_{k \neq l} r_k \xi_{lk} (\rho_s(s_l, s_k) + \rho_a(a_l, a_k))^2 \right] \right. \\
&\quad \left. - \left[\sum_{k \neq l} \xi_l \xi_{lk} (\rho_s(s_l, s_k) + \rho_a(a_l, a_k))^2 \right] \right\} \\
&= \frac{2C}{Z_L} \sum_{k,l} (r_l - \xi_l) (r_k - \xi_l) \xi_{lk} (\rho_s(s_l, s_k) + \rho_a(a_l, a_k))^2,
\end{aligned} \tag{8}$$

where Θ is the parameters of the function f_Θ , r_l is a label (reward) for a state-action pair (node), ξ_l is a predicted label, and we attribute the constant term to C , the goal of training the graph G is to minimize the difference between the predicted labels and their corresponding ground truth labels.

The primary objective is to minimize the difference between the predicted labels ξ_l and their corresponding ground truth labels r_l for state-action pairs (nodes) within the graph G . The equation calculates how changes in the model parameters Θ affect the loss. It starts with a summation symbol, which implies that the gradient is computed by summing up certain terms for all possible l values. Difference between predicted and true labels: The term $(r_l - \xi_l)$ represents the difference between the true label r_l and the predicted label ξ_l for a specific state-action pair l . The next part, $\frac{\partial \xi_l}{\partial \Theta}$, represents the derivative of the predicted label ξ_l with respect to the model parameters Θ . This part shows how small changes in the parameters affect the predicted label. These terms are based on the relationships between labels, the differences between them, and various distance metrics (ρ_s and ρ_a) applied to state and action pairs. The final expression for the gradient involves further calculations and summations over different combinations of

state-action pairs (k and l), as well as the products of reward differences, predicted labels, and the distances between state-action pairs. The equation introduces a constant term C which is attributed to the goal of training the graph G to minimize the difference between predicted and true labels.

APPENDIX B THE PROOF OF REWARD INFERENCE

In this section, we present the proof process for Formula (7). The inference of rewards for unlabelled nodes requires considering the information transfer between labelled and unlabelled nodes, we use $W_{UL}R_L$ for this calculation, while also taking into account the relationships between unlabeled nodes themselves, computed using $W_{UU}R_U$. Since unknown rewards R_U are a variable to be learned, we provide an iterative computation formula by:

$$R_U \leftarrow W_{UU}R_U + W_{UL}R_L. \tag{9}$$

Proof. Let $W_{UL}R_L = \alpha$, then we have

$$R_U^1 \leftarrow W_{UU}R_U^0 + \alpha, \tag{10}$$

where R_U^0 is the initial R_U , and R_U^1 is the result of first iteration. Given the second iteration,

$$R_U^2 \leftarrow W_{UU}(W_{UU}R_U^0 + \alpha) + \alpha, \tag{11}$$

$$R_U^2 \leftarrow W_{UU}^2 R_U^0 + W_{UU}\alpha + \alpha. \tag{12}$$

Given the third iteration,

$$R_U^3 \leftarrow W_{UU}(W_{UU}^2 R_U^0 + W_{UU}\alpha + \alpha) + \alpha, \tag{13}$$

$$R_U^3 \leftarrow W_{UU}^3 R_U^0 + W_{UU}^2 \alpha + W_{UU}\alpha + \alpha. \tag{14}$$

Given the fourth iteration,

$$R_U^4 \leftarrow W_{UU}^4 R_U^0 + W_{UU}^3 \alpha + W_{UU}^2 \alpha + W_{UU}\alpha + \alpha. \tag{15}$$

$$\dots\dots\dots \tag{16}$$

Given the t -th iteration,

$$R_U^t \leftarrow W_{UU}^t R_U^0 + W_{UU}^{t-1} \alpha + \dots + W_{UU}\alpha + \alpha, \tag{17}$$

$$R_U^t \leftarrow W_{UU}^t R_U^0 + (W_{UU}^{t-1} + \dots + W_{UU} + 1)\alpha. \tag{18}$$

□

Based on the weights calculated by Equation (2), the values in W_{UU} are all less than 1. Therefore, as t approaches infinity, W_{UU}^t tends to infinitesimal values, leading $W_{UU}^t R_U^0$ converges to 0.

Meanwhile, $(W_{UU}^{t-1} + \dots + W_{UU} + 1)$ forms a geometric series, and after applying the formula for the sum of a geometric series, we obtain the solution to TRAIN:

$$R_U = (I - W_{UU})^{(-1)} W_{UL}R_L, \tag{19}$$

which is a *fixed point*, and I is the identity matrix [14], [16].

APPENDIX C

DIFFERENT TOTAL PAIRS AND LABELLED PROPORTION FOR EACH TASK

In Table III, we show, for each task, the total number (total) of state-action pairs used to train policies and the ratio of state-action pairs labelled rewards. From the data presented in the table, we can observe that for the majority of tasks, using 10% to 15% of data with rewards is sufficient to achieve completion. Only a small number of complex tasks require 20% of data with rewards to accomplish the task.

TABLE III

FOR EACH TASK, THE TOTAL NUMBER (TOTAL) OF STATE-ACTION PAIRS USED TO TRAIN POLICIES AND THE RATIO OF STATE-ACTION PAIRS LABELLED REWARDS.

| Tasks | Total pairs | Labelled data ratio |
|---------------------------|-----------------|---------------------|
| basketball | 1×10^6 | 15% |
| box-close | 1×10^6 | 10% |
| button-press | 1×10^6 | 15% |
| button-press-topdown | 1×10^6 | 15% |
| button-press-topdown-wall | 2×10^6 | 15% |
| coffee-button | 1×10^6 | 10% |
| coffee-pull | 1×10^6 | 15% |
| dial-turn | 1×10^6 | 15% |
| disassemble | 2×10^6 | 15% |
| door-close | 1×10^6 | 10% |
| door-lock | 1×10^6 | 10% |
| door-open | 1×10^6 | 15% |
| door-unlock | 1×10^6 | 15% |
| drawer-close | 1×10^6 | 10% |
| drawer-open | 1×10^6 | 10% |
| faucet-close | 1×10^6 | 10% |
| faucet-open | 1×10^6 | 10% |
| hammer | 2×10^6 | 10% |
| hand-insert | 2×10^6 | 15% |
| handle-press | 1×10^6 | 15% |
| handle-press-side | 1×10^6 | 10% |
| handle-pull | 1×10^6 | 10% |
| handle-pull-side | 1×10^6 | 10% |
| lever-pull | 1×10^6 | 10% |
| pick-out-of-hole | 2×10^6 | 20% |
| pick-place | 2×10^6 | 15% |
| plate-slide | 1×10^6 | 10% |
| plate-slide-back | 1×10^6 | 10% |
| plate-slide-back-side | 1×10^6 | 10% |
| plate-slide-side | 1×10^6 | 10% |
| push | 1×10^6 | 15% |
| push-back | 1×10^6 | 15% |
| push-wall | 1×10^6 | 15% |
| reach | 1×10^6 | 10% |
| reach-wall | 1×10^6 | 10% |
| stick-pull | 2×10^6 | 20% |
| stick-push | 2×10^6 | 20% |
| sweep | 1×10^6 | 15% |
| sweep-into | 1×10^6 | 15% |
| window-close | 1×10^6 | 10% |
| window-open | 1×10^6 | 10% |
| Cheetah Run | 1×10^6 | 10% |
| Walker Walk | 1×10^6 | 10% |
| Fish Swim | 1×10^6 | 15% |
| Humanoid Run | 1×10^6 | 20% |
| Cartpole Swingup | 1×10^6 | 10% |

APPENDIX D

DISCUSSION

A. computational cost

In this section, we choose to evaluate the computational costs of our method in several experimental environments, including both training time and memory consumption.

Most of our datasets consist of 1×10^6 state-action pairs, equivalent to 1×10^6 nodes in the graph. For computational convenience, we segment the dataset. Our dataset comprises training data from classical reinforcement learning algorithms, such as SAC (Soft Actor-Critic). As the policy learns, different "regions" of the dataset exhibit diversity, with "similar" data typically found within the same segment. Therefore, we have reason to believe that slicing the dataset sequentially is a reasonable approach.

We conducted tests for dataset slices containing 10000 state-action pairs and for dataset slices containing 20000 state-action pairs on a computer with the following specifications: CPU: Intel i9-9900KF 3.6GHz, GPU: RTX 2070 SUPER (8GB VRAM). The training time and memory consumption for the environments are presented in Table IV and Table V.

We also conducted tests for dataset slices containing 30000 state-action pairs and for dataset slices containing 40000 state-action pairs on a server with the following specifications for larger dataset slices: CPU: Intel Xeon Gold 6230 2.10GHz, GPU: RTX 3090 (24GB VRAM). The training time and memory consumption for the environments are presented in Table VI and Table VII.

We anticipate significantly faster computation on server-grade hardware and the ability to use larger slices on GPUs with greater VRAM.

B. Trend in the changes of reward inference values

We examine the changes in the maximum value of R_U to verify whether the learned rewards are bounded by the annotated data. Since R_U is calculated through Formula (7), we design an illustration to demonstrate this issue concerning the formula. We fix R_L as a 3×1 matrix with values $\{1, 2, 3\}$. Meanwhile, for demonstration purposes, we treat $(I - W_{UU})$ and W_{UL} in Formula (7) as two variables, with values ranging from 0.01 to 0.09. The trend of the maximum value in R_U with the variation of $(I - W_{UU})$ and W_{UL} is illustrated in Fig. 10.

From the graph, it can be observed that within certain ranges of $(I - W_{UU})$ and W_{UL} values, the maximum value in R_U can exceed the maximum value in R_L , that is the learned rewards are not bounded by the annotated data.

C. Another Baseline

In the preceding sections, we compared our method with reward learning baselines in the field of offline reinforcement learning. The primary concept of Φ_{GCN} [37] in online reinforcement learning reward learning can also be applied to this scenario.

Upon this baseline, we conducted experimental validations on selected environments. In the experiments, we utilized the

TABLE IV
COMPUTATIONAL COST FOR DATASET SLICES CONTAINING 10000 STATE-ACTION PAIRS.

| Env | Cheetah Run | Walker Walk | Hammer | Door | Pick-place |
|--------------------|-------------|-------------|--------|-------|------------|
| Training time | 12.68s | 12.67s | 2.67s | 2.7s | 2.62s |
| Memory consumption | 2351MB | 2351MB | 2377MB | 2377M | 2377MB |

TABLE V
COMPUTATIONAL COST FOR DATASET SLICES CONTAINING 20000 STATE-ACTION PAIRS.

| Env | Cheetah Run | Walker Walk | Hammer | Door | Pick-place |
|--------------------|-------------|-------------|--------|-------|------------|
| Training time | 14.8s | 13.7s | 13.07s | 13.9s | 13.52s |
| Memory consumption | 5869MB | 5869MB | 5886MB | 5886M | 5886MB |

TABLE VI
COMPUTATIONAL COST FOR DATASET SLICES CONTAINING 30000 STATE-ACTION PAIRS.

| Env | Cheetah Run | Walker Walk | Hammer | Door | Pick-place |
|--------------------|-------------|-------------|---------|--------|------------|
| Training time | 37.61s | 38.07s | 23.12s | 24.34s | 26.72s |
| Memory consumption | 11511MB | 11511MB | 11583MB | 11583M | 11583MB |

TABLE VII
COMPUTATIONAL COST FOR DATASET SLICES CONTAINING 40000 STATE-ACTION PAIRS.

| Env | Cheetah Run | Walker Walk | Hammer | Door | Pick-place |
|--------------------|-------------|-------------|---------|---------|------------|
| Training time | 39.1s | 40.09s | 28.34s | 29.21s | 29.86s |
| Memory consumption | 19577MB | 19577MB | 19691MB | 19691MB | 19691MB |

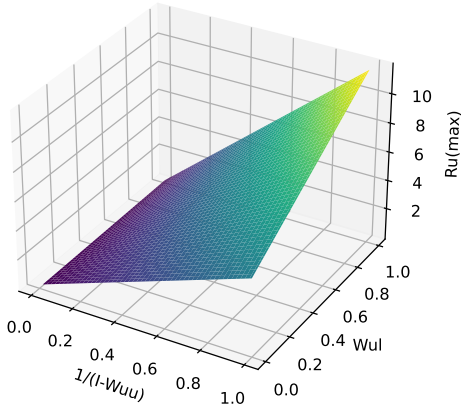


Fig. 10. Trend in the changes of reward inference values.

same data annotation ratio as our approach for Φ_{GCN} . We performed five random seed experiments for each environment, calculating the average and standard deviation of the results. The experimental results are presented in Table VIII and Table IX:

Φ_{GCN} considers information derived from the state and therefore performs well in environments where the state contributes significantly to the reward. For the environments where the action has a substantial impact on the reward, the performance of Φ_{GCN} is slightly inferior.

TABLE VIII
EVALUATION RETURNS ON THE 4 DEEPMIND CONTROL SUITE TASKS. THE AVERAGE \pm STANDARD DEVIATION IS SHOWN FOR FIVE RANDOM SEEDS.

| Env | Cheetah Run | Walker Walk | Fish Swim | Cartpole Swingup |
|--------------|----------------|-------------------|-------------------|------------------|
| TRAIN | 430 \pm 55.9 | 952.7 \pm 155.2 | 567.6 \pm 155.2 | 642.4 \pm 68.9 |
| Φ_{GCN} | 274 \pm 71.1 | 634 \pm 172.3 | 181 \pm 93.2 | 396 \pm 132.1 |

TABLE IX
EVALUATION RETURNS ON THE 5 META-WORLD TASKS. THE AVERAGE \pm STANDARD DEVIATION IS SHOWN FOR FIVE RANDOM SEEDS.

| Env | Coffee Button | Push Wall | Hammer | Open Drawer | Window-open |
|--------------|------------------|------------------|-----------------|-----------------|------------------|
| TRAIN | 4128 \pm 210.9 | 4501 \pm 204.6 | 4532 \pm 59.1 | 4466 \pm 41.3 | 3829 \pm 208.4 |
| Φ_{GCN} | 2845 \pm 303.8 | 3238 \pm 192.1 | 2933 \pm 81.8 | 2989 \pm 79.3 | 2921 \pm 234.1 |